SAND2017-4961J

Extension of the Hugoniot and analytical release model of α-quartz to 0.2 - 3 TPa

M.P. Desjarlais,[1,a] M.D. Knudson,[1,2] and K.R. Cochrane[1]

[1] *Sandia National Laboratories, Albuquerque, New Mexico 87123, USA*

[2] *Institute for Shock Physics, Washington State University, Pullman, Washington 99164-2816, USA*

In recent years, α-quartz has been used prolifically as an impedance matching standard in shock wave experiments in the multi-Mbar regime (1 Mbar = 100 GPa = 0.1 TPa). This is due to the fact that above ~90-100 GPa along the principal Hugoniot α-quartz becomes reflective, and thus shock velocities can be measured to high precision using velocity interferometry. The Hugoniot and release of α-quartz has been studied extensively, enabling the development of an analytical release model for use in impedance matching. However, this analytical release model has only been validated over a range of 300-1200 GPa (0.3-1.2 TPa). Here we extend the range of validity of this analytical model to 200-3000 GPa (0.2-3 TPa) through additional α-quartz Hugoniot and release measurements, as well as first-principles molecular dynamics calculations.

[a] Electronic mail: mpdesja@sandia.gov

I. INTRODUCTION

With the advent of high-energy density facilities, such as large lasers or pulsed power accelerators, shock wave studies have become routine in the multi-Mbar regime (1 Mbar = 100 GPa = 0.1 TPa). The vast majority of these studies rely on an impedance matching (IM) technique, where the shock response of the material of interest is determined through comparison of the shock response of that material with the shock response of a known material standard.

In recent years α-quartz has been used prolifically as an IM standard. This is due to the fact that above ∼90-100 GPa along the principal Hugoniot - the locus of end states achievable through compression by large-amplitude shock waves - α-quartz melts into a conducting fluid with appreciable reflectivity.[1–3] This enables the use of velocity interferometry [VISAR (Ref. 4)] techniques to directly measure the shock velocity to high precision, significantly improving the precision of inferred results using the IM method. However, the accuracy of the inferred shock response of the sample depends upon both the Hugoniot and either the release or reshock response of α-quartz, depending upon the sample's relative shock impedance.

This paper builds upon previous work[5] that utilized α-quartz Hugoniot and release measurements to develop an analytical release model for use in the IM technique. The previous analytical model was validated over a range of 300-1200 GPa (0.3-1.2 TPa). Here we utilize additional α-quartz Hugoniot and release measurements to extend the region of validation to lower pressure (P), and first-principles molecular dynamics (FPMD) calculations to constrain the extrapolation of the model to higher P.

Section II describes the FPMD calculations of the Hugoniot and release in the few TPa regime. The results of additional α-quartz Hugoniot and release experiments are described in Section III. The extension of the Hugoniot and release model for α-quartz is presented in Section IV. The main findings are summarized in Section V.

II. FIRST-PRINCIPLES MOLECULAR DYNAMICS CALCULATIONS OF α-QUARTZ

To extend the Hugoniot and release model of α-quartz to higher P, FPMD calculations were performed using VASP (Vienna *ab-initio* simulation program), a plane-wave density functional theory code developed at the Technical University of Vienna.[6] We used the same method that was reported to be in excellent agreement with plate-impact shock wave experiments on α-quartz using the Z machine,[2] and that used in the development of the recent release model.[5]

Specifically, the silicon and oxygen atoms were represented with projector augmented wave (PAW) potentials[7,8] and exchange and correlation was modeled with the Armiento-Mattsson (AM05) functionals.[9] A total of 72 atoms were included in the supercell, with a plane wave cutoff energy of 600 eV. We note that convergence tests were run with 162 atoms and plane wave cutoff energy of 900 eV, with markedly similar results. Simulations were performed in the canonical ensemble, with simple velocity scaling as a thermostat, and typically covered a few to several picoseconds of real time.

The Rankine-Hugoniot jump conditions,[10] which are derived by considering conservation of mass, momentum, and energy across a steady propagating wave, provide a set of equations relating the initial energy, volume, and pressure with steady state, post-shock values:

$$(E - E_0) = (P + P_0)(V_0 - V)/2 \quad (1)$$

$$(P - P_0) = \rho_0 U_s u_p \quad (2)$$

$$\rho = \rho_0 U_s/(U_s - u_p) \quad (3)$$

where E, P, V, ρ, U_s, and u_p denote the energy, pressure, volume, density, shock velocity, and particle velocity, respectively, and the subscript 0 denotes initial values. The first of these equations, derived from the conservation of energy, provides a prescription for calculation of the Hugoniot. For a given ρ, an initial estimate is made for the temperature, T, or P that would satisfy Eq. 1. A slow T ramp, typically spanning several hundred K about the estimated Hugoniot T, is then applied to the system at a rate of $\sim$1 K/fs. The resulting FPMD simulation allows the determination of P and E for which Eq. 1 is satisfied at the given ρ. Furthermore, the T ramp method also allows for the estimation of both $\Gamma = V(dP/dE)_V$ and the specific heat, which are very useful in estimating the T and P for

TABLE I. AIMD Hugoniot data for α-Quartz. P_0 and ρ_0 were taken to be 1 GPa and 2.644 g/cm^3, respectively. U_s^{quartz} and u_p^{quartz} were then determined from the jump conditions (Eqs. 1-3).

P (TPa)	ρ (g/cm^3)	U_s^{quartz} (km/s)	u_p^{quartz} (km/s)
2.462	8.38	36.87	25.24
3.025	8.70	40.53	28.22

subsequent Hugoniot calculations that are performed when approximating a release path. Hugoniot points at ~2.5 and ~3 TPa calculated in this way are listed in Table I.

A release path from high P was calculated by taking advantage of the fact that at the initial reference state the isentrope and the Hugoniot have a second order contact,[10] which is most easily seen by considering a Taylor series expansion of the entropy as a function of volume. Thus for small volume changes the isentrope is well approximated by the Hugoniot. We therefore approximated the release path as a series of small Hugoniot jumps, where each calculated Hugoniot state along the approximated release path served as the initial reference state for the subsequent Hugoniot calculation. Typical volume jumps were of the order of 5%, resulting in pressure jumps of ~5-10%, with a total of ~12-15 individual calculations along the release path.

A release path calculated in this way from ~3 TPa is shown as the green line in Fig. 1. Also shown for comparison (black line) is a reflection of the α-quartz principal Hugoniot about the particle velocity of the shocked state. Initially the release path drops below the RH, due to the higher sound speed at high P, however at lower pressures the release path crosses above the RH. This is due to the fact that at a given volume, the release path has significantly higher entropy, and therefore increased thermal pressure, than the corresponding state on the RH. For reference, shown as gray lines in Fig. 1, are Hugoniots for several materials that have recently been studied with α-quartz as a standard. For moderate impedance materials, such as CO_2, GDP, and H_2O, the difference between the release path and the RH is ~2% to lower u_p, while for low impedance materials, such as D_2, He, and H_2, the difference can be as large as ~5% to higher u_p.

In accordance with the recent release model for α-quartz[5] we compared the FPMD calculated release path with that from a Mie-Grüneisen (MG) model holding Γ constant, with

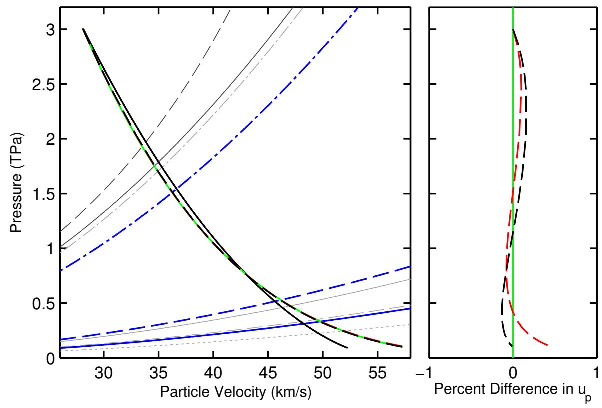

FIG. 1. Comparison of the FPMD release path (green) to the RH (black) and the MGLR release curves for $\Gamma = 0.601$ and $S = 1.213$ (dashed red) and $\Gamma = 0.582$ and $S = 1.197$ (dashed black). Also shown are the Hugoniots of CO_2 (dashed dark gray), GDP (solid dark gray), H_2O (dot-dashed light gray), TPX (dot-dashed blue), 190 mg/cc aerogel (dashed blue), D_2 (solid light gray), He (dashed light gray), 110 mg/cc aerogel (solid blue), and H_2 (dotted light gray). The right panel shows the particle velocity residual of the MGLR release curves with respect to the FPMD.

a linear $U_s - u_p$ Hugoniot response as the reference curve for the MG model; this model is referred to as the MG, linear reference (MGLR) model. The MGLR model has two parameters; Γ and the slope, S, of the linear $U_s - u_p$ Hugoniot ($U_s = C_0 + Su_p$) used for the reference curve. Note that for a given value of S, there is a unique value of C_0 that will produce (P_1, u_{p1}) along the Hugoniot;

$$C_{01} = \frac{P_1}{\rho_0 u_{p1}} - Su_{p1}, \tag{4}$$

where the notation C_{01} explicitly denotes that C_0 is a function of P along the Hugoniot. The values of Γ and S can be simultaneously optimized to minimize the integral:

$$\int_{P_{\min}}^{P_1} (u_p^{\mathrm{rel}}(P') - u_p^{\mathrm{FPMD}}(P'))^2 dP' \tag{5}$$

where u_p^{rel} and u_p^{FPMD} are the particle velocities along the MGLR and FPMD release paths, respectively.

The optimal release path for the MGLR model is shown as the dashed red line in Fig. 1, with $\Gamma = 0.601$ and $S = 1.213$. The MGLR release path with these values of Γ and S agrees quite well with the calculated FPMD release path, as can be seen by the particle velocity

TABLE II. Values for Γ and S for the MGLR model for both cases (i) Γ, S optimized, and (ii) Γ optimized and S fixed.

P_H	U_s	Γ, S optimized		Γ optimized	
(TPa)	(km/s)	Γ	S	Γ	S
0.306	14.492	0.205	1.189	0.220	1.197
0.408	16.486	0.356	1.198	0.355	1.197
0.537	18.508	0.447	1.190	0.457	1.197
0.805	22.126	0.578	1.211	0.558	1.197
1.048	25.034	0.592	1.205	0.580	1.197
3.007	40.530	0.601	1.213	0.582	1.197

residual with respect to the FPMD release path shown in the right panel of Fig. 1. Note that the value of S obtained from the optimization is similar to that found at lower P (see Table II). It was also found that there exists a broad, shallow minimum in the evaluated integral (Eq. 5) along a line in Γ-S space, as illustrated in Fig. 2. This broad minimum is what enabled the simplification of the reported MGLR model,[5] allowing S to be held constant, thereby reducing the model to a single free parameter, Γ. Using the value of $S = 1.197$ (the same as that used in the recent release model[5]) results in an optimized value of $\Gamma = 0.582$. The corresponding release curve is shown in Fig. 1 as the dashed black line. Note that there is a negligible degradation in agreement between the MGLR and FPMD release paths with $S = 1.197$ (see also Fig. 2), suggesting that the previous analytical model with $S = 1.197$ can be suitably extended to P in the few TPa range.

III. EXPERIMENTAL α-QUARTZ MEASUREMENTS

A series of planar, plate-impact, shock wave experiments were performed at the Sandia Z machine[11] to obtain additional Hugoniot data for α-quartz and to extend the experimental release measurements of α-quartz to lower P. The experimental configuration used is the same as that described in Ref. 5. Silica aerogel with initial density of $\sim$190 mg/cm^3 was used as a low-impedance standard. The shock response of the aerogel has been previously investigated on the Z machine through plate-impact, shock wave experiments.[12,13] Since the

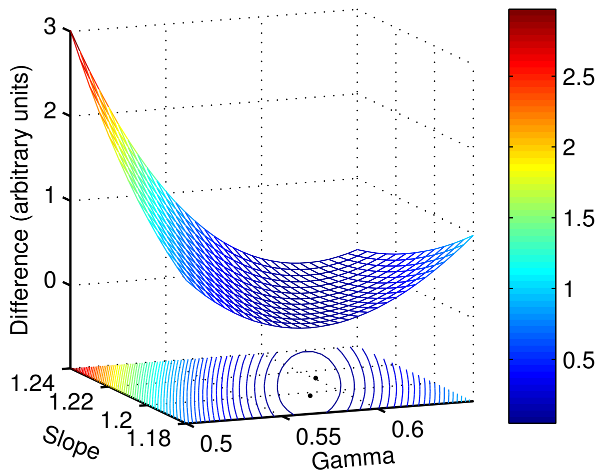

FIG. 2. Integrated difference between the MGLR and the FPMD release path (Eq. 5) from ∼3 TPa as a function of both Γ and S. Note the shallow minimum along a line in Γ-S space. The black circles on the Γ-S plane correspond to both cases (i) Γ, S optimized, and (ii) Γ optimized and S fixed.

TABLE III. Silica aerogel, aluminum, and copper $U_s - u_p$ coefficients and covariance matrix elements[5]

	C_0 (km/s)	S	$\sigma^2_{C_0}$ (x10^{-2})	σ^2_S (x10^{-4})	$\sigma_{C_0}\sigma_S$ (x10^{-3})
$\sim$ 190 mg/cm^3 aerogel	−0.385	1.248	2.631	2.710	−1.493
Aluminum	6.322	1.189	5.358	4.196	−4.605
Copper	4.384	1.382	1.344	6.084	−2.689

aerogel is solid, it could be directly impacted by the flyer-plate, and thus the Hugoniot states could be inferred through simple IM with aluminum under compression, to relatively high-precision. The linear $U_s - u_p$ coefficients and covariance matrix elements for the aerogel, which were used in the analysis of the release experiments described here, are listed in Table III.

The α-quartz (single-crystal, z-cut, obtained from Argus International) and ∼190 mg/cm^3 silica aerogel (fabricated by General Atomics) samples were all nominally 5 mm in lateral dimension. The thickness of the α-quartz was nominally 300 microns, while the thicknesses of the silica aerogel was nominally 1000 microns. The aerogel samples were metrologized using a measuring microscope to determine sample diameters and an interferometer to measure thickness to a precision of ∼5 microns and less than 1 micron, respectively. Density of the silica aerogel was inferred from high-precision mass measurements and inferred volume assuming the samples were right-circular cylinders. Slight departure from the right-circular cylinder assumption resulted in density uncertainty of ∼2%.

The α-quartz samples and silica aerogel were glued together to form experimental "stacks" using the techniques described in Ref. 5. The flyer-plates and experimental "stacks" were diagnosed using a velocity interferometer (VISAR[4]). Since all of the materials in the "stacks" are transparent, the 532 nm laser light could pass through the "stack" and reflect off the flyer-plate surface. This allowed an in-line measurement of the flyer-plate velocity from initial motion to impact. Upon impact a shock wave of several 100 GPa was sent through the α-quartz sample. This shock was of sufficient magnitude that the shocked α-quartz became weakly reflective in the visible range. This immediate onset of reflectivity allowed for direct measurement of the shock velocity within the α-quartz using the VISAR diagnostic. Upon traversal of the α-quartz sample, the shock was transmitted into the silica aerogel and a substantial release wave was reflected back into the α-quartz sample. The resulting 10's of GPa shock in the silica aerogel was of sufficient magnitude that it also became weakly reflecting, allowing direct measure of the shock velocity in the silica aerogel with the VISAR diagnostic.

The measured apparent velocity of the shock in the α-quartz and silica aerogel was reduced by a factor equal to the refractive index of the unshocked material: $v = v_a/n_0$. The values of n_0 used in this study for α-quartz and silica aerogel was 1.547 and 1.038, respectively.[14–16] Ambiguity in the fringe shift upon both impact and transition of the shock velocity measurement from the α-quartz sample to the silica aerogel was mitigated through the use of three different VISAR sensitivities, or velocity per fringe (vpf) settings at each measurement location, included a high sensitivity vpf setting of 0.2771 km/s/fringe. We conservatively estimate the resolution of the VISAR system at one tenth of a fringe, resulting in uncertainty in flyer-plate and shock velocities of a few tenths of a percent.

The flyer velocity immediately before impact and the α-quartz shock velocity immediately after impact enabled a Hugoniot measurement through the IM method described in Ref. 2. The linear $U_s - u_p$ coefficients and covariance matrix elements for the aluminum and copper, which were used in the analysis of the Hugoniot experiments described here, are listed in Table III.

The α-quartz release experiments were analyzed within the framework of the MGLR model. The measured U_s^{quartz} and known α-quartz Hugoniot[2,5] defined the initial state in the $P - u_p$ plane, (P_1, u_{p1}). The measured shock velocity and the known Hugoniot of the silica aerogel[13] defined the release state (P_r, u_{pr}) along the α-quartz release path. The MGLR model, with $S = 1.197$, was then used to determine the value of Γ_{eff} such that the release path emanating from (P_1, u_{p1}) went through the point (P_r, u_{pr}). Uncertainties in the inferred quantities were determined using the Monte Carlo method described in Ref. 5. Note that the uncertainty in u_{pr} that arises from both the uncertainty of the silica aerogel Hugoniot[13] and the measured shock velocity is less than 1%, and provides a tight constraint on the value of Γ_{eff} that connects (P_1, u_{p1}) and (P_r, u_{pr}). This translates into an uncertainty in Γ_{eff} of between 0.05 and 0.1 for the individual measurements. We note that because (i) n_0 for the aerogel samples is common to both the direct impact experiments and the release experiments, and (ii) the shock impedance of the silica aerogel is so much lower than the shock impedance of α-quartz, Γ_{eff} is only weakly dependent on n_0 and the estimated 1% uncertainty in n_0 for the aerogel does not contribute significantly to the uncertainty in Γ_{eff}.

A total of 9 α-quartz Hugoniot points were obtained in this study. The pertinent parameters for these measurements displayed in Table IV. Additionally, four α-quartz release measurements were performed using ~190 mg/cm^3 silica aerogel as the standard to extend the empirical release model to lower P. The pertinent parameters for these experiments are listed in Table V. Finally, we note that in finalizing the TPX Hugoniot publication[17] it was discovered that in the analysis of experiment Z2332 an incorrect number of fringe jumps was used for both the Hugoniot measurement (correct values listed in Ref. 17) and the release measurement (compare Table V in Ref. 5 with Table VI here). Also, a more precise value for the refractive index of TPX was used ($n_0 = 1.461$) resulting in slightly higher inferred values of U_s^{TPX} in the release experiments. The revised values for Γ_{eff} for TPX are listed in Table VI.

TABLE IV. $U_s - u_p$ Hugoniot data for α-quartz. The impactor material is listed in the flyer column, with 'Al' and 'Cu' designating aluminum and copper, respectively. v_f and U_s^{quartz} are the measured flyer-plate and quartz shock velocity, respectively. u_p^{quartz}, P, and ρ are the inferred quartz particle velocity, pressure, and density in the shocked state, respectively. $\sigma^2_{U_s}$, $\sigma^2_{u_p}$, and $\sigma_{U_s}\sigma_{u_p}$ are the covariance matrix elements that describe the correlation between the uncertainties in U_s and u_p.

Expt	flyer	v_f (km/s)	U_s^{quartz} (km/s)	u_p^{quartz} (km/s)	$\sigma^2_{U_s}$ (x10^{-3})	$\sigma^2_{u_p}$ (x10^{-3})	$\sigma_{U_s}\sigma_{u_p}$ (x10^{-4})	P (GPa)	ρ (g/cm^3)
Z2877	Cu	8.89 ± 0.05	12.01	6.16	1.600	1.586	-1.914	195.9 ± 1.4	5.44 ± 0.04
Z2858	Al	14.59 ± 0.05	14.02	7.54	1.600	1.424	-3.176	280.2 ± 1.5	5.73 ± 0.04
Z2858	Al	14.77 ± 0.05	14.16	7.63	1.600	1.411	-3.262	286.0 ± 1.5	5.74 ± 0.04
Z2858	Al	15.93 ± 0.05	14.96	8.19	1.600	1.367	-3.323	324.7 ± 1.5	5.86 ± 0.04
Z2586	Al	16.72 ± 0.05	15.51	8.57	1.600	1.343	-3.340	352.4 ± 1.6	5.93 ± 0.04
Z2690	Al	26.97 ± 0.05	22.23	13.61	1.600	1.437	-3.601	801.8 ± 2.4	6.84 ± 0.04
Z2690	Al	28.91 ± 0.05	23.52	14.56	1.600	1.564	-3.601	907.3 ± 2.7	6.95 ± 0.04
Z2577	Al	31.59 ± 0.05	25.02	15.93	1.600	1.835	-3.654	1056.0 ± 3.1	7.29 ± 0.04
Z2577	Al	31.84 ± 0.05	25.34	16.01	1.600	1.881	-3.782	1075.3 ± 3.2	7.20 ± 0.04

TABLE V. Γ_{eff} for the α-quartz release experiments using $\sim$190 mg/cm^3 silica aerogel as a standard. U_s^{Q}, U_s^{gel}, and ρ_0^{gel} are the measured shock velocities of the α-quartz and aerogel samples, and the measured aerogel initial density.

Expt	U_s^{Q} (km/s)	U_s^{gel} (km/s)	ρ_0^{gel} (mg/cm^3)	Γ_{eff}
Z2877N	11.07 ± 0.03	10.97 ± 0.03	194 ± 4	-0.182 ± 0.097
Z2877S	12.02 ± 0.03	12.20 ± 0.03	194 ± 4	-0.135 ± 0.076
Z2858N	14.02 ± 0.03	15.06 ± 0.03	190 ± 4	0.060 ± 0.051
Z2858S	15.10 ± 0.04	16.70 ± 0.04	190 ± 4	0.175 ± 0.059

TABLE VI. Updated $\Gamma_{\rm eff}$ for the α-quartz release experiments using TPX as a standard. $U_s^{\rm Q}$, $U_s^{\rm TPX}$, and $\rho_0^{\rm TPX}$ are the measured shock velocities of the α-quartz and TPX samples, and the measured TPX initial density (Compare this Table with Table V from Ref. 5).

Expt	$U_s^{\rm Q}$ (km/s)	$U_s^{\rm TPX}$ (km/s)	$\rho_0^{\rm TPX}$ (g/cm^3)	$\Gamma_{\rm eff}$
Z2436	15.69 ± 0.03	17.67 ± 0.03	0.83 ± 0.004	0.264 ± 0.085
Z2450N	16.30 ± 0.03	18.47 ± 0.03	0.83 ± 0.004	0.377 ± 0.077
Z2450S	17.45 ± 0.03	19.94 ± 0.03	0.83 ± 0.004	0.476 ± 0.068
Z2345N	20.45 ± 0.03	23.84 ± 0.03	0.83 ± 0.004	0.577 ± 0.051
Z2345S	21.69 ± 0.03	25.50 ± 0.03	0.83 ± 0.004	0.599 ± 0.046
Z2333N	22.00 ± 0.03	25.92 ± 0.03	0.83 ± 0.004	0.604 ± 0.045
Z2333S	22.97 ± 0.03	27.21 ± 0.03	0.83 ± 0.004	0.595 ± 0.041
Z2375	25.19 ± 0.03	30.12 ± 0.03	0.83 ± 0.004	0.530 ± 0.039
Z2332	25.45 ± 0.03	30.63 ± 0.03	0.83 ± 0.004	0.607 ± 0.040

IV. EXTENSION OF HUGONIOT AND RELEASE MODEL FOR α-QUARTZ

The experimental Hugoniot measurements from this study (red diamonds) are plotted along with the previous experimental results[2,5] (blue crosses) and fit[5] (dashed black line) in Fig. 3. These results are in good agreement with both the previous published data and fit. Also plotted in Fig. 3 are the two FPMD calculated Hugoniot points at ∼2.5 and ∼3 TPa (green diamonds). In contrast, the FPMD results exhibit shock velocities that are systematically higher than the extrapolation of the previous fit, suggesting that the extrapolation is too compressible, with a slope that is slightly too low.

Comparison of the FPMD calculations with experiment over the P range of 100-1200 GPa (0.1-1.2 TPa) demonstrate that the FPMD calculations are within 1% throughout this entire range (see Fig. 2 in Ref. 2), with the largest difference being in the P range where the molecular fluid undergoes dissociation into an atomic fluid. This level of agreement suggests the FPMD calculations accurately describes the hot dense fluid, particularly at higher P where the effects of disorder and dissociation of the molecular fluid become less significant,

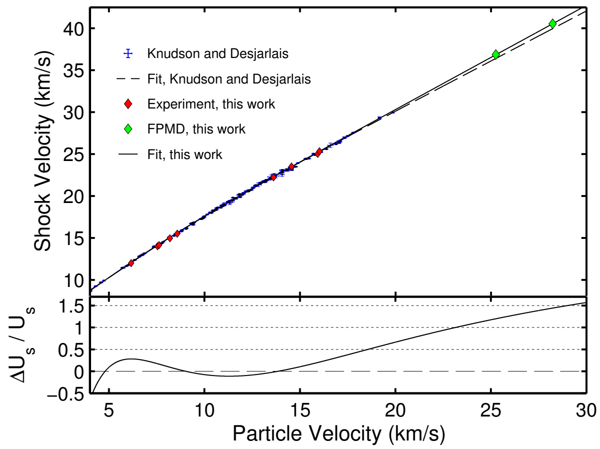

FIG. 3. α-quartz U_s-u_p Hugoniot. Blue crosses, previous experimental results;[2,5] red (green) diamonds, present experimental (FPMD) results; solid (dashed) black line, present (previous) fit. The bottom panel shows the residual of the present fit to the previous fit.

and that the FPMD results in the few TPa range can be used to constrain the extrapolation of the fit to the experimental U_s-u_p data.

We therefore performed a new least squares, weighted fit using the same functional form as that in Ref. 2:

$$U_s = a + b\,u_p - c\,u_p\,e^{-d u_p} \tag{6}$$

A weighting factor of 1/300 (fractional uncertainty of a few tenths of a percent, similar to that of the experimental data) was chosen such that the percent uncertainty in the fit at high P was of the same order as that of the previous fit in the P range (below about 1 TPa) constrained by the experimental data (see Fig. 4). The coefficients and covariance matrix elements for the new fit are listed in Tables VII and VIII, respectively. The difference between the previous fit and the new fit is less than 0.5% over the particle velocity range for which experimental data exists, as can be seen in the bottom panel of Fig. 3. However, at higher P, in the few TPa range, the difference grows to over 1% due to the difference in their asymptotic slopes (1.193 and 1.242 for the previous[5] and new fit, respectively). When used for IM in the TPa regime, this behavior would tend to result in an inferred response that is systematically too compressible when using the previous fit (the inferred u_p would be too high for a given U_s).

The experimental Γ_{eff} values from the $\sim$190 mg/cm^3 aerogel (Table V) and the revised Γ_{eff} values from the previous TPX release experiments (Table VI) are plotted along with

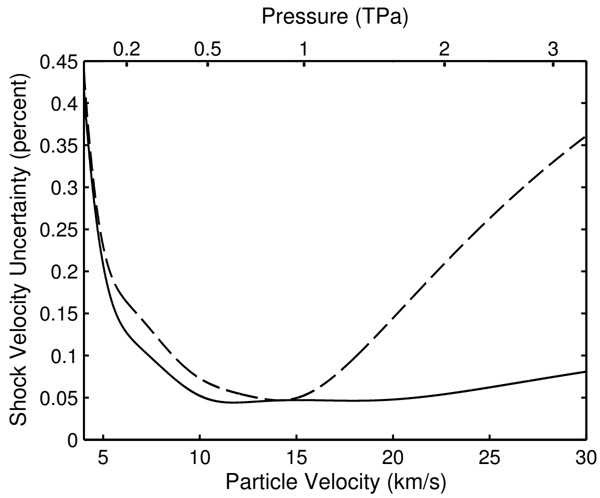

FIG. 4. Percent uncertainty in U_s for a given u_p for the previous (dashed line) and current (solid line) U_s-u_p fits.

TABLE VII. Coefficients for the α-quartz $U_s - u_p$ relation displayed in Eq. 6

	a	b	c	d
	(km/s)			$(\text{km/s})^{-1}$
α-quartz	5.477	1.242	2.453	0.4336

the previously reported[5] Γ_{eff} values for both ∼110 and ∼190 mg/cm^3 silica aerogel in Fig. 5. Also shown in Fig. 5 are the Γ_{eff} values determined from the FPMD release calculations. In general there is good agreement between the FPMD results and experiment, with the possible exception being at low P (∼300 GPa) where the FPMD results appear to exhibit a slightly lower slope than experiment. However, this P range corresponds to the region where the effects of disorder and dissociation are the most significant[2] and where the largest difference is seen between the experimental and FPMD Hugoniots. As was the case for the Hugoniot, at high P the agreement between experiment and FPMD becomes much better.

TABLE VIII. Covariance matrix elements for the α-quartz $U_s - u_p$ relation displayed in Eq. 6

	σ_a^2	$\sigma_a\sigma_b$	$\sigma_a\sigma_c$	$\sigma_a\sigma_d$	σ_b^2	$\sigma_b\sigma_c$	$\sigma_b\sigma_d$	σ_c^2	$\sigma_c\sigma_d$	σ_d^2
	(x10^{-3})	(x10^{-4})	(x10^{-3})	(x10^{-4})	(x10^{-6})	(x10^{-4})	(x10^{-5})	(x10^{-2})	(x10^{-3})	(x10^{-4})
α-quartz	3.028	−1.490	−3.715	−6.275	7.839	1.448	2.752	1.729	1.605	1.907

In particular, the Γ_{eff} value determined from the FPMD release calculation from ∼3 TPa suggests a saturation in Γ_{eff} at high P. The experimental data from this study at low P (below 300 GPa) provide a much needed constraint on the dependence of Γ_{eff} at lower P in the region of dissociation.

The experimental data and the highest P FPMD datum were fit to a piecewise function that was constrained to have a second order contact at the breakpoint; see Eq. 7. These data were adequately fit with a linear function at lower U_s^{Q} and the same exponential function as in Ref. 5 at higher U_s^{Q}:

$$\Gamma_{\text{eff}} = \begin{cases} -1.4545 + 0.1102\, U_s^{\text{Q}} \pm 0.036, & U_s^{\text{Q}} \leq 14.69 \\ 0.579\left(1 - \exp\left[-0.129\left(U_s^{\text{Q}} - 12.81\right)^{3/2}\right]\right) \pm 0.036, & U_s^{\text{Q}} > 14.69. \end{cases} \tag{7}$$

We note that the fit was essentially unchanged with and without inclusion of the FPMD value at ∼3 TPa. The uncertainty in Γ_{eff} was determined through an analysis of the standard deviation of the measured values with respect to the value given by Eq. 7; this analysis resulted in an uncertainty in Γ_{eff} of 0.036, as shown in Fig. 5. Note that the previous fit for Γ_{eff} from Ref. 5 (gray line), is within the uncertainty of the new fit.

V. CONCLUSION

The previously published Hugoniot[2,5] and release model[5] for α-quartz has been extended, and is now validated over the P range of 0.2-3 TPa. This was accomplished through experimental Hugoniot and release measurements (to extend the release model to lower P) and FPMD calculations of the Hugoniot and release of α-quartz in the few TPa range (to extend the Hugoniot fit to higher P). The FPMD Hugoniot calculations indicated that the asymptotic slope of the fit to the experimental U_s-u_p data was too low, and were used to constrain the extrapolation of the fit to the few TPa range. The α-quartz release measurements at lower P (between 200-300 GPa) provided a much needed constraint on the dependence of Γ_{eff} at lower P, in the region of dissociation.

The extension to the analytical model will result in negligible differences in inferred quantities with respect to the previous model when used for IM in the 0.3-1.2 TPa range. However, when used for IM in the few TPa range the new model will result in lower inferred u_p for a given U_s. This difference is expected to be ∼1-2% in u_p which corresponds to ∼3-8%

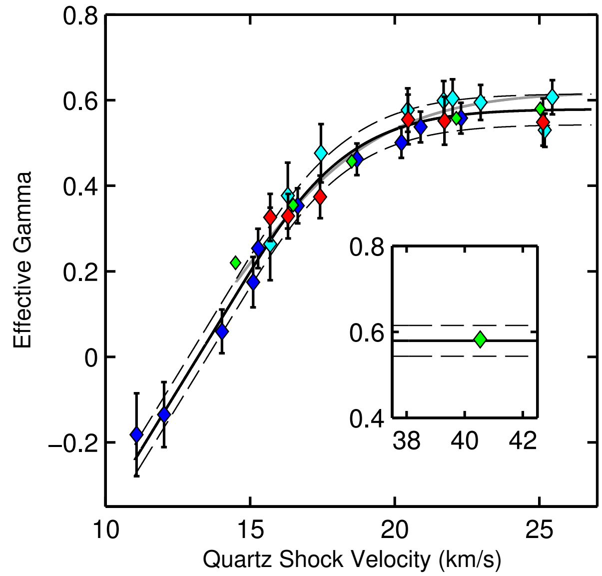

FIG. 5. Γ_{eff} as a function of U_s^{Q}. Cyan diamonds, TPX standard; blue (red) diamonds, $\sim$190 ($\sim$110) mg/cm^3 silica aerogel standard; green diamonds, FPMD derived values; solid (dashed) black line, best fit (one σ deviation) to the experimental data; solid gray line, best fit from Ref. 5. Note that the x and y scales of the inset match the main figure.

lower inferred ρ, given that the error in ρ scales as roughly $(\rho/\rho_0 - 1)$ times the error in u_p (in this P regime ρ/ρ_0 is $\sim$4-5). While this model is now validated to $\sim$3 TPa, we anticipate that the model can be extrapolated to higher P with some confidence; in this regime the P is sufficiently high that the effects of disordering and dissociation in the shocked fluid are becoming much less significant and the behavior of the system is approaching that of an ideal gas.

ACKNOWLEDGMENTS

The authors would like to thank the large team at Sandia that contributed to the design and fabrication of the flyer-plate loads and the fielding of the shock diagnostics. Sandia National Laboratories is a multiprogram laboratory managed and operated by Sandia Corporation, a wholly owned subsidiary of Lockheed Martin Corporation, for the U.S. Department of Energys National Nuclear Security Administration under Contract No. DE-AC04-94AL85000.

REFERENCES

[1] D. G. Hicks, T. R. Boehly, P. M. Celliers, J. H. Eggert, E. Vianello, D. D. Meyerhofer, and G. W. Collins, Phys. Plasmas **12**, 082702 (2005).

[2] M. D. Knudson and M. P. Desjarlais, Phys. Rev. Lett. **103**, 225501 (2009).

[3] D. G. Hicks, T. R. Boehly, J. H. E. J. E. Miller, P. M. Celliers, and G. W. Collins, Phys. Rev. Lett. **97**, 025502 (2006).

[4] L. M. Barker and R. E. Hollenbach, J. Appl. Phys. **43**, 4669 (1972).

[5] M. D. Knudson and M. P. Desjarlais, Phys. Rev. B **88**, 184107 (2013).

[6] G. Kresse and J. Furthmüller, Phys. Rev. B **54**, 11169 (1996).

[7] P. E. Blöchl, Phys. Rev. B **50**, 17953 (1994).

[8] G. Kresse and D. Joubert, Phys. Rev. B **59**, 1758 (1999).

[9] R. Armiento and A. E. Mattsson, Phys. Rev. B **72**, 085108 (2005).

[10] G. E. Duvall and R. A. Graham, Rev. Mod. Phys. **49**, 523 (1977).

[11] M. Matzen *et al.*, Phys. Plasmas **12**, 055503 (2005).

[12] M. D. Knudson, J. R. Asay, and C. Deeney, J. Appl. Phys. **97**, 073514 (2005).

[13] M. D. Knudson and R. W. Lemke, J. Appl. Phys. **114**, 053510 (2013).

[14] G. G. Ghosh, Opt. Commun. **163**, 95 (1999).

[15] A. Danilyuk *et al.*, Nucl. Instr. and Meth. A **494**, 491 (2002).

[16] D. Richter and D. Lipka, Nucl. Instr. and Meth. A **513**, 635 (2003).

[17] S. Root, T. R. Mattsson, K. Cochrane, R. W. Lemke, and M. D. Knudson, J. Appl. Phys. **118**, 205901 (2015).